Cooperative communication with regenerative relays for cognitive radio networks

Tuan Do and Brian L. Mark
Dept. of Electrical and Computer Engineering
George Mason University, MS 1G5
4400 University Drive, Fairfax, VA
email: tdoa@gmu.edu, bmark@gmu.edu

***Abstract*—Cognitive radios hold tremendous promise for increasing spectral efficiency in wireless systems. In cognitive radio networks, secondary users equipped with frequency-agile cognitive radios communicate with one another via spectrum that is not being used by the primary, licensed users of the spectrum. We consider a cooperative communication scenario in which a secondary transmitter can communicate with a secondary receiver via a direct communication link or a relay channel, depending on the state of a primary transmitter. We develop a decode-and-forward transmission strategy that exploits the presence of spectrum holes both in time and in space. A strategy based on pure temporal sensing alone uses the direct link when the primary transmitter is off, whereas a scheme based on spatial sensing alone uses the relay channel. Our numerical results show that the proposed scheme, employing joint spatial-temporal sensing, significantly reduces the average symbol error probability compared to schemes based on pure temporal or pure spatial sensing.**

***Index Terms*—Cognitive radio, cooperative communications, dynamic spectrum access**

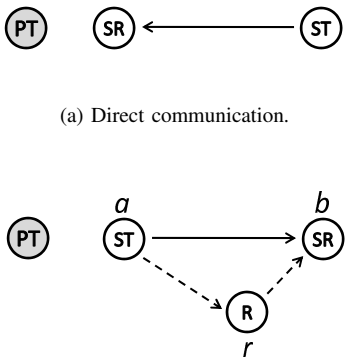

(a) Direct communication.

(b) Cooperative communication.

Fig. 1. Joint spatial-temporal sensing via cooperative communication.

I. Introduction

As the proliferation of wireless devices and applications continues to grow, the demand for spectrum resources keeps increasing. In the current spectrum regulatory framework, spectrum or frequency is allocated to licensed users over a geographic area. Within these constraints, spectrum is considered a scarce resource due to static spectrum allocation. Empirical studies of radio spectrum usage have shown that licensed spectrum is typically highly under-utilized [1], [2]. To recapture the so-called "spectrum holes," various schemes for allowing unlicensed or secondary users to opportunistically access unused spectrum have been proposed. Opportunistic or dynamic spectrum access is achieved by cognitive radios that are capable of sensing the radio environment for spectrum holes and dynamically tuning to different frequency channels to access them. Such radios are often called *frequency-agile* or *spectrum-agile*.

On a given frequency channel, a spectrum hole can be characterized as spatial or temporal. A *spatial* spectrum hole can be specified in terms of the maximum transmission power that a secondary user can employ without causing harmful interference to primary users that are receiving transmissions from another primary user that is transmitting on the given channel. Spatial spectrum sensing is investigated [3], wherein the maximum interference-free transmit power (MIFTP) of a given secondary user is estimated based on signal strengths received by a group of secondary nodes. To calculate the MIFTP for a secondary node, estimates of both the location and transmit power of the primary transmitter are computed collaboratively by a group of secondary nodes. Using these estimates, each secondary node determines its approximate MIFTP, which bounds the size of its spatial spectrum hole.

A *temporal* spectrum hole is a period of time for which the primary transmitter is idle. During such idle periods, a secondary user may opportunistically transmit on the given channel without causing harmful interference. The problem of detecting when the primary is ON or OFF is called *temporal* spectrum sensing. Cooperative temporal sensing has been studied in [4], [5]. The decision on the ON/OFF status of the primary transmitter can be made either at individual secondary nodes or collaboratively by a group of secondary nodes. In [6], a temporal spectrum sensing strategy that exploits multiuser diversity among secondary nodes is proposed.

In an earlier paper [7], a joint spatial-temporal sensing was proposed. In the proposed scheme, a secondary node performs spatial sensing to determine its MIFTP when the primary transmitter is ON and uses localization information obtained in the process of spatial sensing to improve the performance of temporal sensing, which estimates the ON/OFF state of the primary transmitter.

In this paper[1], we propose a cooperative communication strategy with regenerative (decode-and-forward) relays that employ joint spatial-temporal spectrum sensing to maximize the transmission capacity of secondary users in a cognitive radio network. In Fig. 1(a), the secondary transmitter (ST), labeled as node a, can communicate directly with the secondary receiver (SR), labeled as node b, due to the existence of a spatial spectrum hole with respect to the primary transmitter (PT). However, in the scenario depicted in Figs. 1(b), ST can communicate directly with SR only when PT is in the OFF state. In this scenario, when PT is ON, ST transmits to SR via a relay (R), labeled as node r. By enabling the use of both the direct and relay channels, joint spatial-temporal sensing can significantly improve the transmission performance of the secondary systems.

Cooperative communications and diversity have received a lot of attention in recent years (cf. [8]–[11]). Two well-known cooperative strategies are amplify-and-forward (AF) and decode-and-forward (DF). The non-regenerative AF strategy achieves diversity via maximal ratio combining [9] and requires storage of analog waveforms at relay nodes. The regenerative DF strategy is simple and practical but cannot achieve full diversity unless sophisticated combining is employed at the destination to account for the unreliability of the link from the source to the relay and the link from the relay to the destination [9]. In [10], a smart DF strategy is proposed to achieve available diversity.

In [12], an AF strategy is proposed for cognitive radio network scenario wherein the status of primary transmitter is ON for a greater proportion of time than OFF, on average. It is assumed that the secondary receiver has to wait until it receives signals from both the relay and the secondary transmitter to decode the received signals. This may result in excessive delay on the communication link.

In this paper, we propose a practical cooperative communication protocol for cognitive radio networks based on the DF strategy. Our protocol decodes the received signals after three time frames. No constraints are placed on the ON/OFF activity of the primary transmitter, i.e., the proportion of time spent in the ON state may be greater or less than that in the OFF state. We focus on the case of a single relay channel.

The remainder of the paper is organized as follows. Section II describes the system model. Section III discusses the performance of the system. Section IV presents simulation results. Finally, the paper is concluded in Section V.

II. System Model

We assume the basic system configuration shown in Fig. I. For convenience, we label ST as a, SR as b, and R as r.

A. Transmission frames and PT behavior

We assume that time on the wireless channel is divided into frames consisting of N_s symbols each. We shall assume perfect symbol-level timing synchronization between the nodes of the secondary system. The case of imperfect synchronization has been studied in [11]. The PT alternates between the ON and OFF states on a per-frame basis according to the on-off Markov model of Fig. 2.

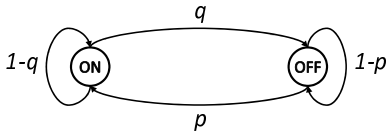

Fig. 2. Two-state Markov chain model for PT ON/OFF process.

The ON and OFF durations of PT are modeled as geometric random variables with parameters p and q, respectively (cf. [13]). The steady-state probability that PT is ON is given by $p_{\rm on} = p/(p+q)$, while the probability that PT is OFF is $p_{\rm off} = q/(p+q)$. In [12], we considered the scenario in which on average, PT in the ON state a greater proportion of time than in the OFF state, i.e., $p > q$. In this paper, this restriction is removed.

B. Channel modeling

The received signal of a simple wireless channel model with flat (frequency non-selective) fading without shadowing is given by [14]

$$y = \sqrt{P(d,\epsilon)}hs + n, \tag{1}$$

where

$$P(d,\epsilon) \triangleq \delta^2 \left(\frac{d_0}{d}\right)^{\alpha} \epsilon$$

denotes the equivalent transmitted power after taking into account the effect of path loss. Here, δ^2 is the free space signal-power attenuation factor between the source and a reference distance d_0, d is the distance between the source and destination, α is the propagation exponent, $h \sim \mathcal{CN}(0,1)$ is a complex Gaussian random variable with variance 1, $n \sim \mathcal{CN}(0, N_0)$, and s is the transmitted signal.

When PT is ON, ST and R are limited in the amount of power they can use in order to avoid causing harmful interference to the primary users who receive the transmissions from PT. The maximum power that can be used by a given secondary node while avoiding harmful interference to primary users is called the *maximum interference-free transmit power* (MIFTP) (cf. [3], [15]). A method for a secondary node to estimate its MIFTP is presented in [3] for the case of a single primary transmitter; the multiple transmitter case is addressed in [16]. Let ϵ_a and ϵ_r denote the MIFTPs of ST and R, respectively, when PT is ON. We also define

$$P_{ar} = P(d_{ar}, \epsilon_a),\ P_{rb} = P(d_{rb}, \epsilon_r),$$

as the equivalent transmitted powers when PT is ON from ST to R and from R to SR, respectively. Here, d_{ar} and d_{rb} denote the distances between the node pairs (ST, R) and (R, SR), respectively. For the case when PT is OFF, we define

$$\tilde{P}_{ab} = P(d_{ab}, \epsilon_m),\ \tilde{P}_{ar} = P(d_{ar}, \epsilon_m),\ \tilde{P}_{rb} = P(d_{rb}, \epsilon_m),$$

[1]This work was supported in part by the U.S. National Science Foundation under Grants CNS-0520151 and ECS-0246925.

as the equivalent transmitted powers from ST to SR, ST to R, and R to SR, respectively. Here, d_{ab} denotes the distance between ST and SR and ϵ_m denotes the maximum transmit power that secondary nodes can use when PT is OFF.

In a cognitive radio network where $\epsilon_a \ll \epsilon_m$, ST may not be able to communicate directly with ST when PT is ON because P_{ar} could be below the required threshold for SR to detect the received signal. In this case, ST can communicate with SR through the relay node R, since $d_{ar} < d_{ab}$.

C. Decode-and-Forward Cooperative Transmission

We develop a general decode-and-forward (DF) cooperative transmission protocol for cognitive radio networks. We assume that both ST and R employ omnidirectional antennas. The secondary receiver (SR) decodes received signals once every three time frames. Suppose the secondary transmitter (ST) desires to transmit N_s symbols to ST; i.e., it requires one full frame in which PT is OFF. We assume that a time division multiple access (TDMA) protocol is used to coordinate the transmissions of ST and R. During a given time frame, only ST or R is allowed to transmit to SR.

The DF cooperative protocol works as follows:

- In the first two time frames, if PT is OFF, ST transmits to SR. Otherwise, ST transmits to R.
- In the third time frame, R transmits to SR.

In order to achieve this, the secondary nodes perform joint spatial-temporal sensing, as discussed in [7]. In particular, all secondary users estimate their MIFTPs based on signal strength measurements, which they exchange with one another. They also decide whether the PT is ON or OFF by transmitting their local decisions to a fusion center, which then makes the final decision. Maximal ratio combining (MRC) is used at both R and SR to combine the received signals.

The state of PT over three consecutive time frames can be characterized by a three-bit state sequence $c_1c_2c_3$ where $c_i = 1$ if PT is ON during the ith frame and $c_i = 0$, otherwise. Therefore, there are $2^3 = 8$ possible state sequences. During a frame in which PT is OFF, the ST communicates directly with SR using the maximum transmission power ϵ_m. Since an omnidirectional antenna is used at ST, the relay node R receives the signal transmitted by ST. Let $\mathbf{c}$ denote a sequence of frame states and let $|\mathbf{c}|$ denote the length of the sequence.

For a given state sequence $\mathbf{c}$, let $w_{\mathbf{c}}$, $u_{\mathbf{c}}$ and $v_{\mathbf{c}}$ denote the signals received at SR for link (ST, SR), at R for link (ST, R) and at SR for link (R, SR), respectively, at the end of the $|\mathbf{c}|$-th frame. For example, u_{10} denotes the received signal at R due to source ST after two time frames, where PT is ON in the first frame and OFF in the second. Let $y_{c_1c_2c_3}$ denote the final MRC-received signal (i.e., the signal is obtained using MRC) at SR after three time frames. For example y_{000} is the MRC-received signal at SR after a sequence of three time frames in which PT is OFF during all three frames.

Let f_i, g_i and h_i denote the channel fading coefficients during time frame i ($i = 1, 2, 3$) from ST to SR, ST to R and R to SR, respectively. We assume that f_i, g_i and h_i are constant and independently identically distributed from one frame to another. Further, the channel states f_i and h_i are available at SR, i.e., via training sequences, but they are not available at ST and R. Also, the g_i are available at R, but not at ST. Hence, maximum likelihood detection can be used at R and SR. Let s be the transmitted signal at ST and s_d the decoded signal at R. Let n_i be the noise variable during time frame i, $i = 1, 2, 3$.

Consider the state sequence 000. During the first two time frames, ST transmits the same signal to SR using a repetition code [17]. After the second frame, the received signal at SR from ST is

$$w_{00} = \sqrt{\tilde{P}_{ab}} \sum_{i=1}^{2} |f_i|^2 s + \sum_{i=1}^{2} f_i^* n_i,$$

where x^* denotes the complex conjugate of x and the received signal at R is

$$u_{00} = \sqrt{\tilde{P}_{ar}} \sum_{i=1}^{2} |g_i|^2 s + \sum_{i=1}^{2} g_i^* n_i.$$

In the third time frame, R decodes u_{00} to obtain s_d and then forwards s_d to SR. The received signal at SR from R is

$$v_{000} = \sqrt{\tilde{P}_{rb}} h_3 s_d + n_3.$$

The final received signal at SR after MRC is

$$y_{000} = w_{00} + h_3^* v_{000} \tag{2}$$

For state sequence 001, the received signal at SR from ST after the first two time frames is

$$w_{00} = \sqrt{\tilde{P}_{ab}} \sum_{i=1}^{2} |f_i|^2 s + \sum_{i=1}^{2} f_i^* n_i.$$

Due to the use of the repetition code, the received signal at relay R after MRC over the first two time frames is u_{00}. The relay decodes u_{00} and forwards s_d to SR during the third time frame when PT is ON. The received signal at SR from R after the third frame is

$$v_{001} = h_3 \sqrt{P_{rb}} s_d + n_3.$$

The final received signal at SR after MRC is

$$y_{001} = w_{00} + h_3^* v_{001}. \tag{3}$$

Consider state sequence 010. During the first time frame, ST transmits the signal

$$w_0 = \sqrt{\tilde{P}_{ab}} f_1 s + n_1$$

to SR. In the second time frame, ST transmits this signal to R. The received signal at R after two time frames is

$$u_{01} = \left(\sqrt{\tilde{P}_{ar}} |g_1|^2 + \sqrt{P_{ar}} |g_2|^2 \right) s + g_1^* n_1 + g_2^* n_2.$$

The relay R then decodes and forwards the decoded signal s_d to SR, so that

$$v_{010} = \sqrt{\tilde{P}_{rb}} h_3 s_d + n_3.$$

The final received signal at SR is given by

$$y_{010} = f_1^* t_0 + h_3^* v_{010}. \tag{4}$$

For the remaining state sequences, the final signal received at SR can be derived similarly. The results are given as follows:

$$y_{011} = f_1^* w_0 + h_3^* v_{011}, \qquad v_{011} = \sqrt{P_{rb}} h_3 s_d + n_3, \quad (5)$$

$$y_{100} = f_2^* w_{10} + h_3^* v_{100}, \qquad v_{100} = \sqrt{\tilde{P}_{rb}} h_3 s_d + n_3, \quad (6)$$

$$y_{101} = h_3^* v_{101} + f_2^* w_{10}, \qquad v_{101} = h_3 \sqrt{P_{rb}} s_d + n_3, \quad (7)$$

$$y_{110} = h_3^* v_{110}, \qquad v_{110} = h_3 \sqrt{\tilde{P}_{rb}} s_d + n_3, \quad (8)$$

$$y_{111} = h_3^* v_{111}, \qquad v_{111} = h_3 \sqrt{P_{rb}} s_d + n_3. \quad (9)$$

D. Pure spatial and pure temporal sensing models

The pure spatial sensing model is equivalent to the case when PT is ON at all times, i.e., the state sequence is 111. Therefore, the received signal at SR in the case of pure spatial sensing is given by $y^s = y_{111} = h_3^* v_{111}$. In pure temporal sensing, the transmission strategy is a simple repetition code over the time frames in which PT is OFF. The received signal at SR under pure temporal sensing for the eight possible state sequences can be derived as follows:

$$y^t_{000} = \sqrt{\tilde{P}_{ab}} \sum_{i=1}^{3} |f_i|^2 s + \sum_{i=0}^{3} f_i^* n_i,$$

$$y^t_{001} = \sqrt{\tilde{P}_{ab}} \sum_{i=1}^{2} |f_i|^2 s + \sum_{i=0}^{2} f_i^* n_i,$$

$$y^t_{010} = (|f_1|^2 + |f_3|^2)\sqrt{\tilde{P}_{ab}} s + f_1^* n_1 + f_3^* n_3,$$

$$y^t_{011} = |f_1|^2 \sqrt{\tilde{P}_{ab}} s + f_1^* n_1,$$

$$y^t_{100} = (|f_2|^2 + |f_3|^2)\sqrt{\tilde{P}_{ab}} s + f_2^* n_2 + f_3^* n_3,$$

$$y^t_{101} = |f_2|^2 \sqrt{\tilde{P}_{ab}} s + f_2^* n_2,$$

$$y^t_{110} = |f_3|^2 \sqrt{\tilde{P}_{ab}} s + f_3^* n_3.$$

Note that there is no transmission for the state sequence 111, in which PT is ON during all three frames.

The spectral efficiencies for joint-spatial temporal sensing and spatial sensing are equal. The spectral efficiency of temporal sensing is smaller than that of joint spatial-temporal sensing because there is no transmission during state sequence 111. If the joint spatial-temporal sensing scheme has a spectral efficiency of 1 then the temporal sensing has an efficiency of $1 - p_{\text{on}}^3$ where p_{on} is the steady-state probability that PT is ON during a given frame.

III. Performance analysis

We analyze the performance of decode-and-forward strategy in terms of symbol error probability (SEP).

A. Joint spatial-temporal sensing

Let denote $\text{SEP}_{\mathbf{c}}$ denote the SEP under state e sequence $\mathbf{c} = c_1 c_2 c_3$ and let SEP denote the SEP averaged over all possible state sequences for joint spatial-temporal sensing. Under the system model discussed in Section II, the average SEP can be obtained as

$$\begin{aligned}\text{SEP} = [&p_{\text{off}}^3 \text{SEP}_{000} + p_{\text{off}}^2 p_{\text{on}} (\text{SEP}_{001} + \text{SEP}_{010} + \text{SEP}_{100}) \\ &+ p_{\text{off}} p_{\text{on}}^2 (\text{SEP}_{011} + \text{SEP}_{101} + \text{SEP}_{110}) + p_{\text{on}}^3 \text{SEP}_{111}].\end{aligned} \quad (10)$$

We shall assume that M-PSK modulation is used. Using the moment generating function approach in [18], [19], the SEP of M-PSK signals with MRC of L independent fading paths can be expressed as

$$\frac{1}{\pi} \int_0^{\frac{(M-1)\pi}{M}} \prod_{k=1}^{L} M_{\gamma_k} \left(-\frac{g_{\text{PSK}}}{\sin^2 \phi} \right) \mathrm{d}\phi, \quad (11)$$

where $g_{\text{PSK}} = \sin^2(\pi/M)$ and $M_{\gamma_l}(u) = (1 - u\gamma_l)^{-1}$ is the moment generating function of Rayleigh fading with average signal-to-noise ratio (SNR) γ_l. Let $\mathbf{\Gamma} = (\gamma_1, \gamma_2, \ldots, \gamma_L)$ denote a vector of L average SNR values corresponding to L independent fading paths. Then the SEP can be expressed as

$$\psi(\boldsymbol{P}) = \frac{1}{\pi} \int_0^{\frac{(M-1)\pi}{M}} \prod_{k=1}^{L} \left(1 + \frac{g_{\text{PSK}}}{\sin^2 \phi} \gamma_k \right)^{-1} \mathrm{d}\phi. \quad (12)$$

Let $\hat{S}_d$ denote the signal decoded at relay SR. Let $\tilde{\gamma}_{ab} = E\big[|f_i|^2 \frac{\tilde{P}_{ab}}{N_0}\big] = \frac{\tilde{P}_{ab}}{N_0}$ be the average SNR at SR when the transmitter is ST. Define $\gamma_{rb} = E\big[|h_i|^2 \frac{P_{rb}}{N_0}\big] = \frac{P_{rb}}{N_0}$ and $\tilde{\gamma}_{rb} = E\big[|h_i|^2 \frac{\tilde{P}_{rb}}{N_0}\big] = \frac{\tilde{P}_{rb}}{N_0}$ to be the average SNR at SR when the transmitter is the relay R when PT is ON and OFF, respectively Let s_k denote the kth signal in the M-PSK signal constellation, $k = 1, \ldots, M$. For state sequence 000, the received signal is given by (2) and the SEP can be expressed as

$$\text{SEP}_{000} = \Pr[\hat{S}_d = s_k] \cdot \text{SEP}_{000|\hat{S}_d = s_k} + \Pr[\hat{S}_d \neq s_k] \cdot \text{SEP}_{000|\hat{S}_d \neq s_k},$$

where s_k is the transmitted signal $k = 1, 2, \ldots M$,

$$\Pr[\hat{S}_d = s_k] = 1 - \psi(\tilde{\gamma}_{ar}, \tilde{\gamma}_{ar}), \ \Pr[\hat{S}_d \neq s_k] = \psi(\tilde{\gamma}_{ar}, \tilde{\gamma}_{ar}),$$

are the probabilities of successful and unsuccessful decoding at the relay, respectively. Here,

$$\text{SEP}_{000|\hat{S}_d = s_k} = \psi(\tilde{\gamma}_{ab}, \tilde{\gamma}_{ab}, \tilde{\gamma}_{rb})$$

is the SEP under state sequence 000 given that $\hat{S}_d = s_k$, and $\text{SEP}_{000|\hat{S}_d \neq s_k}$ is the SEP given that $\hat{S}_d \neq s_k$. The SEP for state sequence 000 can then be written as

$$\begin{aligned}\text{SEP}_{000} = &[1 - \psi(\tilde{\gamma}_{ar}, \tilde{\gamma}_{ar})] \psi(\tilde{\gamma}_{ab}, \tilde{\gamma}_{ab}, \tilde{\gamma}_{rb}) \\ &+ \psi(\tilde{\gamma}_{ar}, \tilde{\gamma}_{ar}) \cdot \text{SEP}_{000|\hat{S}_d \neq s_k}.\end{aligned} \quad (13)$$

Since $\tilde{\gamma}_{ar} \gg \tilde{\gamma}_{ab}$, $\psi(\tilde{\gamma}_{ar}, \tilde{\gamma}_{ar}) \to 0$ as $\tilde{\gamma}_{ab} \to \infty$. Therefore, for sufficiently large $\tilde{\gamma}_{ab}$, the right hand side of (13) is dominated by the first term. Thus, in this case we have

$$\text{SEP}_{000} \approx [1 - \psi(\tilde{\gamma}_{ar}, \tilde{\gamma}_{ar})] \psi(\tilde{\gamma}_{ab}, \tilde{\gamma}_{ab}, \tilde{\gamma}_{rb}).$$

The validity of this approximation is confirmed in Section IV, where we show simulation results that match well with the results from the analytical approximation.

Using a similar approach as that for the sequence 000, expressions for SEP corresponding to the sequences 001 to 101 can be obtained as follows:

$$\begin{aligned}
\text{SEP}_{001} &\approx [1-\psi(\tilde{\gamma}_{ar},\tilde{\gamma}_{ar})]\psi(\tilde{\gamma}_{ab},\tilde{\gamma}_{ab},\gamma_{rb}),\\
\text{SEP}_{010} &\approx [(1-\psi(\tilde{\gamma}_{ar},\gamma_{ar})]\psi(\tilde{\gamma}_{ab},\tilde{\gamma}_{rb}),\\
\text{SEP}_{011} &\approx [1-\psi(\tilde{\gamma}_{ar},\gamma_{ar})]\psi(\tilde{\gamma}_{ab},\gamma_{rb}),\\
\text{SEP}_{100} &\approx [(1-\psi(\gamma_{ar},\tilde{\gamma}_{ar})]\psi(\tilde{\gamma}_{ab},\tilde{\gamma}_{rb}),\\
\text{SEP}_{101} &\approx [1-\psi(\gamma_{ar},\tilde{\gamma}_{ar})]\psi(\tilde{\gamma}_{ab},\gamma_{rb}).
\end{aligned}$$

Let $\hat{S}$ denote the decoded signal at SR. For state sequence 110, we have

$$\text{SEP}_{110}=\Pr[\hat{S}=s_k]\cdot\text{SEP}_{110|\hat{S}_d=s_k}+\Pr[\hat{S}_d\neq s_k]\Pr[\hat{S}\neq s_k].$$

Given that $S_d \neq s_k$, we have $\Pr[\hat{S} \neq s_k] = \Pr[\hat{S} = s_d]$ for BPSK signals. For M-PSK signals with $M \geq 4$,

$$\Pr[\hat{S}\neq s_k]=\Pr[\hat{S}=s_d]+\sum_{i\neq d,i\neq k}\Pr[\hat{S}=s_i]. \qquad (14)$$

The second term on the right hand side of (14) is the probability that ST erroneously decodes the signal given that the transmitted signal from R is s_d. In practice, the probability is on the order of $10^{-\kappa}$, where $\kappa \geq 3$ is a constant. The probability of correct detection at SR given that s_d is transmitted from the relay, is $\Pr[\hat{S} = s_d]$ and is on the order of $1 - 10^{-\kappa}$ where $\kappa \geq 3$. Thus, $\Pr[\hat{S} \neq s_k] \approx \Pr[\hat{S} = s_d]$. Hence, we find that

$$\begin{aligned}
\text{SEP}_{110} &= [1-\psi(\gamma_{ar},\gamma_{ar})]\psi(\tilde{\gamma}_{rb})+\psi(\gamma_{ar},\gamma_{ar})[1-\psi(\tilde{\gamma}_{rb})],\\
\text{SEP}_{111} &= [1-\psi(\gamma_{ar},\gamma_{ar})]\psi(\gamma_{rb})+\psi(\gamma_{ar},\gamma_{ar})[1-\psi(\gamma_{rb})].
\end{aligned}$$

B. Pure spatial and pure sensing

Pure spatial sensing is equivalent to the scenario given by state sequence 111. Hence, the SEP under pure spatial sensing is $\text{SEP}^s = \text{SEP}_{111}$. The SEP under pure temporal sensing is

$$\begin{aligned}
\text{SEP}^t = \frac{1}{(p+q)^3-p^3}[&q^3\text{SEP}^t_{000}+q^2p(\text{SEP}^t_{001}+\text{SEP}^t_{010}\\
&+\text{SEP}^t_{100})+qp^2(\text{SEP}^t_{011}+\text{SEP}^t_{101}+\text{SEP}^t_{110})],
\end{aligned}$$

where $\text{SEP}^t_{000} = \psi(\tilde{\gamma}_{ab},\tilde{\gamma}_{ab},\tilde{\gamma}_{ab})$, $\text{SEP}^t_{001} = \text{SEP}^t_{010} = \text{SEP}^t_{100} = \psi(\tilde{\gamma}_{ab},\tilde{\gamma}_{ab})$ and $\text{SEP}^t_{101} = \text{SEP}^t_{110} = \text{SEP}^t_{011} = \psi(\tilde{\gamma}_{ab})$. Hence,

$$\begin{aligned}
\text{SEP}^t = \frac{1}{(p+q)^3-p^3}[&q^3\psi(\tilde{\gamma}_{ab},\tilde{\gamma}_{ab},\tilde{\gamma}_{ab})\\
&+3q^2p\psi(\tilde{\gamma}_{ab},\tilde{\gamma}_{ab})+3qp^2\psi(\tilde{\gamma}_{ab})].
\end{aligned}$$

IV. Numerical Results

In this section, we investigate the performance of the proposed decode-and-forward cooperative communication scheme in terms of SEP. The simulation code was implemented using MATLAB. We assume that the channel fading coefficients f_i, g_i, $h_i \sim \mathcal{CN}(0,1)$ $(i = 1,2,3)$, the frame length $N_s = 100$ symbols. We also assume that $\tilde{\gamma}_{ab} = \gamma_{ar} = \gamma_{rb}$, $\tilde{\gamma}_{ar} = \tilde{\gamma}_{rb} = \tilde{\gamma}_{ab} + 10$ dB, and we define $\text{SNR} = \tilde{\gamma}_{ab}$.

In Fig. 3, we compare the performance of pure temporal sensing and spatial sensing with that of joint spatial temporal-sensing with $p = q = 0.5$ and BPSK modulation. We observe

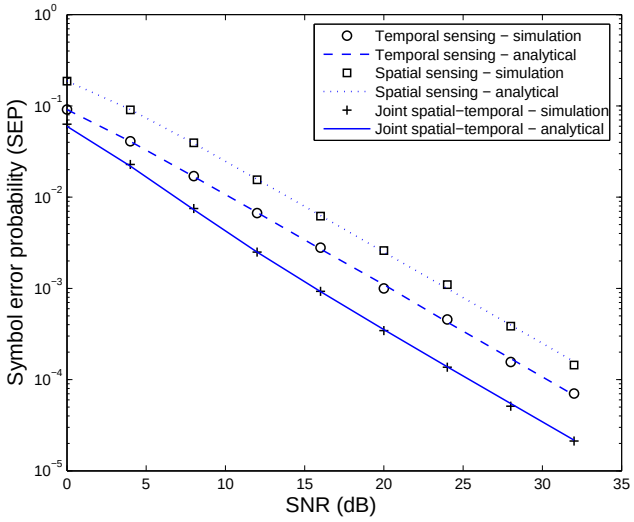

Fig. 3. Performance of cooperative communication with BPSK modulation

that the simulation and analytical results match well with each other. From Fig. 3, we see that the performance of the proposed DF cooperative transmission strategy with joint spatial-temporal sensing is about 10 dB and 6 dB better than that of pure spatial sensing and temporal sensing, respectively. Also the joint spatial-temporal sensing has better spectral efficiency than pure temporal sensing by a factor of $1/(1-p^3) = 1.142$.

In Fig. 4, we compare the performance of spatial sensing, temporal sensing, and joint spatial-temporal cooperative sensing for different values of $p_{\text{off}} = q/(p+q)$ and $\text{SNR} = 16$ dB. Joint spatial-temporal sensing outperforms both spatial sensing and temporal sensing for all values of p_{off}. Note that when $p_{\text{off}} = 1$, the joint spatial-temporal scheme is equivalent to pure temporal sensing, whereas when $p_{\text{off}} = 0$, joint spatial-temporal is equivalent to pure spatial sensing.

Fig. 5 compares the spectral efficiencies of the different sensing strategies. The spectral efficiencies of spatial sensing and joint-spatial sensing are the same and are normalized as 1. As we can see, the spectral efficiency of temporal sensing is smaller than that of joint spatial-temporal sensing. When $p_{\text{off}} = 0$, there is no transmission for temporal sensing, implying that the spectral efficiency is zero in this case.

Fig. 6 shows the performance of the different schemes with QPSK modulation and $p = q = 0.5$. The simulation and analytical results show close agreement. Note that the performance of our DF cooperative transmission strategy with joint spatial sensing is about 10 dB and 6 dB better than that of pure spatial sensing and temporal sensing, respectively when $\text{SEP} = 10^{-3}$.

V. Conclusion

We proposed a cooperative communication protocol with regenerative relays for opportunistic spectrum access in cognitive radio networks. Our protocol combines joint spatial-temporal spectrum sensing and relaying to increase the transmission capacity of cognitive radio networks. Both simulation

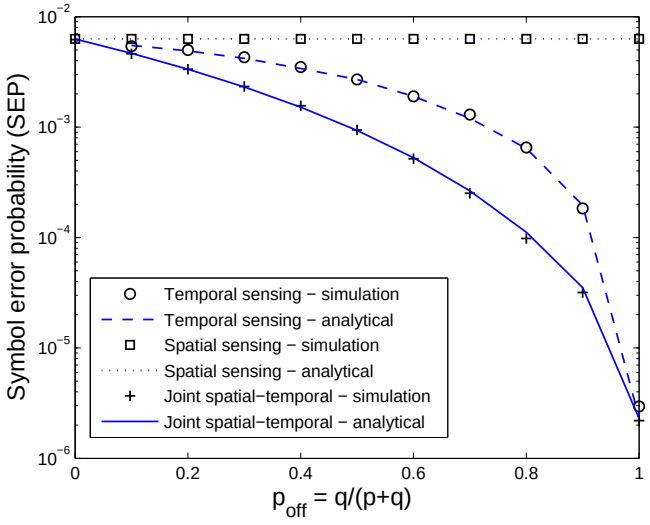

Fig. 4. Performance of cooperative communication with BPSK modulation vs. $q/(p+q)$.

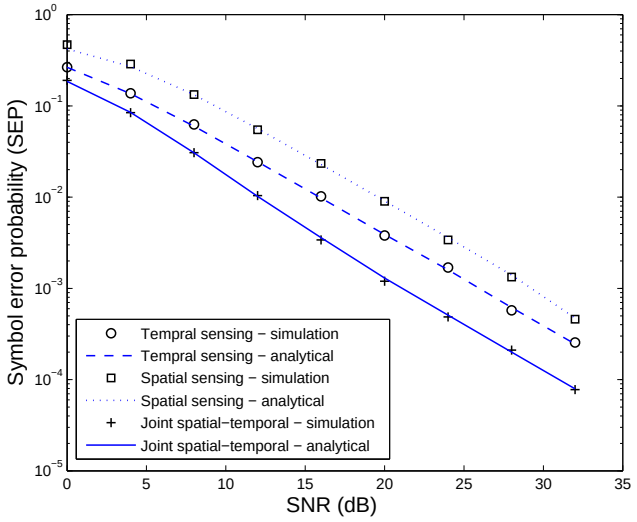

Fig. 6. Performance of cooperative communication with QPSK modulation.

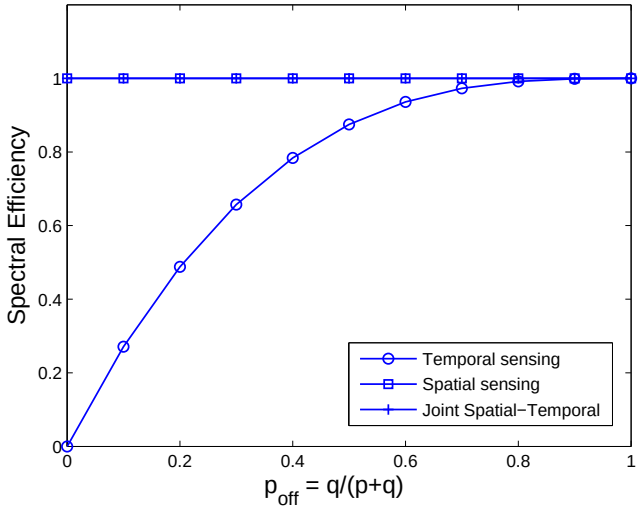

Fig. 5. Spectral efficiency of joint spatial-temporal sensing.

and analytical results confirm that the proposed scheme outperforms schemes based on pure spatial sensing or pure temporal sensing alone. We assumed that knowledge of channel state information was available, hence enabling coherent detection at both the relay and at the secondary receiver. In ongoing work, we are investigating the fast fading scenario wherein noncoherent detection is used at both the relay and the secondary receiver.

REFERENCES

[1] FCC, "Spectrum policy task force," ET Docket 02-135, Nov. 2002.

[2] M. McHenry, "Frequency agile spectrum access technologies," in *FCC Workshop on Cognitive Radio*, May 2003.

[3] B. L. Mark and A. O. Nasif, "Estimation of maximum interference-free transmit power level for opportunistic spectrum access," *IEEE Trans. Wireless Commun.*, vol. 8, no. 5, pp. 2505–2513, 2009.

[4] S. Mishra, A. Sahai, and R. W. Brodersen, "Cooperative sensing among cognitive radios," in *Proc. IEEE Int. Conf. Communications*, vol. 4, Istanbul, Jun. 2006, pp. 1658–1663.

[5] J. Unnikrishnan and V. Veeravalli, "Cooperative sensing for primary detection in cognitive radio," *IEEE J. Sel. Topics Signal Process.*, vol. 2, no. 1, pp. 18–27, Feb. 2008.

[6] T. Do and B. L. Mark, "Expoiting multiuser diversity for spectrum sensing in cognitive radio networks," in *Proc. IEEE Radio and Wireless Symposium*, New Orleans, Jan. 2010.

[7] ——, "Joint spatial-temporal spectrum sensing for cognitive radio networks," in *Proc, Conf. on Information Sciences and Systems (CISS'09)*, Baltimore, MD, Mar. 2009.

[8] J. N. Laneman and G. W. Wornell, "Distributed space-time-coded protocols for exploiting cooperative diversity in wireless networks," *IEEE Trans. Inf. Theory*, vol. 49, no. 10, pp. 2415–2425, Oct. 2003.

[9] J. N. Laneman, D. N. C. Tse, and G. W. Wornell, "Cooperative diversity in wireless networks: Efficient protocol and outage behavior," *IEEE Trans. Inf. Theory*, vol. 50, no. 12, pp. 3062–3080, Dec. 2004.

[10] T. Wang, G. B. Giannakis, and R. Wang, "Smart regenerative relays for link-adaptive cooperative communications," *IEEE Trans. Commun.*, vol. 56, no. 11, pp. 1950–1960, Nov. 2008.

[11] S. Wei, D. Goeckel, and M. Valenti, "Asynchronous cooperative diversity," *IEEE Trans. Wireless Commun.*, vol. 6, no. 6, pp. 1547–1557, 2006.

[12] T. Do and B. L. Mark, "Combining cooperative relaying with spectrum sensing in cognitive radio networks," in *Proc. IEEE Radio and Wireless Symposium*, New Orleans, Jan. 2010.

[13] A. Motamedi and A. Bahai, "MAC protocol design for spectrum-agile wireless networks: Stochastic control approach," in *Proc. IEEE DySPAN'07*, April 2007, pp. 448–451.

[14] J. Boyer, D. D. Falconer, and H. Yanikomeroglu, "Multihop diversity in wireless relaying channels," *IEEE Trans. Commun.*, vol. 52, no. 10, pp. 1820–1830, Oct. 2004.

[15] A. E. Leu, M. McHenry, and B. L. Mark, "Modeling and analysis of interference in listen-before-talk spectrum access schemes," *Int. J. Network Mgmt*, vol. 16, pp. 131–141, 2006.

[16] A. O. Nasif and B. L. Mark, "Opportunistic spectrum sharing with multiple cochannel primary transmitters," *IEEE Trans. Wireless Commun.*, vol. 8, no. 11, pp. 5702–5710, Nov. 2009.

[17] D. Tse and P. Viswanath, *Fundamentals of Wireless Communication*. Cambridge University Press, 2005.

[18] M. K. Simon and M.-S. Alouini, *Digital Communication over Fading Channels*, 2nd ed. Wiley Interscience, 2004.

[19] M.-S. Alouini and A. J. Goldsmith, "A unified approach for calculating error rates of linearly modulated signals over generalized fading channels," *IEEE Trans. Commun.*, vol. 47, no. 9, pp. 1324–1334, 1999.